

Recoil-gated plunger lifetime measurements in ^{188}Pb

A. Dewald, R. Peusquens, B. Saha, P. von Brentano, A. Fitzler, and T. Klug
Institut für Kernphysik, Universität zu Köln, Köln, Germany

I. Wiedenhöver,* M. P. Carpenter, A. Heinz, R. V. F. Janssens, F. G. Kondev,
 C. J. Lister, D. Seweryniak, and K. Abu Saleem
Argonne National Laboratory, 9700 South Cass Avenue, Argonne, Illinois 60439, USA

R. Krücken,† J. R. Cooper,‡ C. J. Barton,§ K. Zyromski, C. W. Beausang, and Z. Wang
W. A. Wright Nuclear Laboratory, Yale University, New Haven, Connecticut 06520, USA

P. Petkov
Institute for Nuclear Research and Nuclear Energy, Sofia, Bulgaria

A. M. Oros-Peusquens||
Georgia Institute of Technology, School of Physics, Atlanta, Georgia 30332-0430, USA

U. Garg and S. Zhu
University of Notre Dame, Notre Dame, Indiana 46556-5670, USA
 (Received 2 June 2003; published 18 September 2003)

Electromagnetic transition probabilities were measured using the recoil distance Doppler-shift technique and the $^{40}\text{Ca}(^{152}\text{Sm},4n)^{188}\text{Pb}$ reaction at a beam energy of 805 MeV to investigate shape coexistence in ^{188}Pb . For the first time, a plunger was combined with Gammasphere and the Argonne Fragment Mass Analyzer. It was possible to measure the lifetimes of two states in the prolate band of ^{188}Pb and, thus, provide for the first time evidence for the collectivity of this band. A three-level mixing calculation revealed that the first 2^+ state is predominantly of prolate character.

DOI: 10.1103/PhysRevC.68.034314

PACS number(s): 21.10.Tg, 23.20.Lv, 27.70.+q

I. INTRODUCTION

The Pb region offers a good illustration of the phenomenon of shape coexistence [1]. While ^{208}Pb is an example of a double-magic spherical nucleus, the first two excited states in the neutron midshell nucleus ^{186}Pb are 0^+ levels for which oblate and prolate deformation can be inferred [2]. Almost as spectacular is the situation in ^{188}Pb , where the 0^+ state of presumed oblate deformation is the first excited state [3,4], followed by the prolate 0^+ excitation, 120 keV higher and almost at the same excitation energy as the 2_1^+ state [5–7].

Two complementary approaches contribute to the theoretical understanding of shape coexistence in the Pb region. In a schematic shell-model approach [8,9], the occurrence of intruder states is explained by the combined effect of (i) the monopole and quadrupole interaction acting in the valence

space of many-particle many-hole (mp-nh) proton excitations across the $Z=82$ closed shell and of (ii) a very large open neutron shell. Qualitatively, the deformation of the mp-nh excitations arises from the deformation-driving quadrupole interactions between the valence protons and neutrons. The behavior with mass of the energy of the first excited 0^+ states in the Pb isotopes is well reproduced. At neutron midshell, the number of valence particles and, thus, the effect of the proton-neutron interaction becomes maximal, and the 2p-2h and 4p-4h configurations are both predicted to be close to the 0p-0h closed shell ground state [9]. In a very different picture, calculations using a deformed mean-field approach [10] show the existence of three closely spaced minima with spherical, oblate ($\beta_2 \approx -0.18$) and prolate ($\beta_2 \approx 0.27$) deformation in the potential energy surfaces of the Pb isotopes around $N=104$. The mean-field approach reproduces well the mass behavior of the first excited 0^+ states, which are associated with the oblate minimum, and predicts the appearance of prolate states at low energies for isotopes below ^{190}Pb .

The experimental study of the light Pb nuclei makes use of two complementary approaches as well. The 0^+ states were successfully studied in the α decay of Po parents, and the reported small hindrance factors [3–6] are consistent with the shell-model mp-nh structure of the levels involved. Furthermore, information obtained from α -decay studies indicates that the properties of the proton shell closure at $Z=82$ do not change significantly in any of the known Pb

*Present address: Florida State University, Physics Department, Tallahassee, FL 32306-4350.

†Present address: Physik-Department E12, TU München, 85748 Garching, Germany.

‡Present address: Lawrence Livermore National Laboratory, Livermore, CA 94550-9234.

§Present address: CCLRC Daresbury Laboratory, Daresbury Warrington Cheshire WA4 4AD, UK.

||Present address: FZ Jülich, D- 52425 Jülich, Germany.

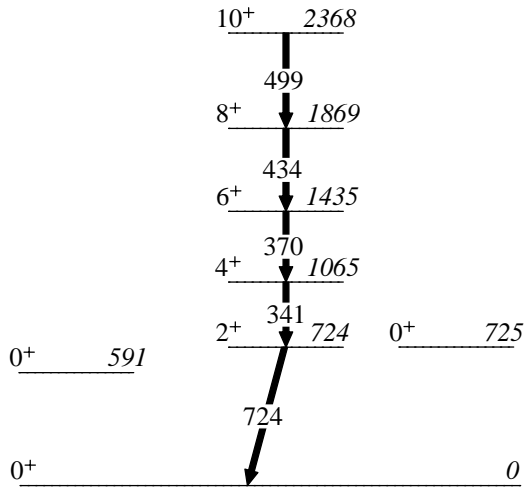


FIG. 1. Partial level scheme of ^{188}Pb adopted from Ref. [12]. The excited 0^+ states are taken from Ref. [7]. The energies are given in keV.

isotopes [4,11], leading to the expectation of spherical character for closed shell nuclei. Experimental evidence concerning low-lying rotational bands in the midshell Pb isotopes, which are expected to be associated with the two deformed 0^+ configurations, has been first provided several years ago for ^{188}Pb and ^{186}Pb [12,13]. The level scheme of ^{188}Pb investigated by Heese *et al.* [12] displays rotational-like sequences, based on a state of spin (2^+), extending up to a (16^+) level. A partial level scheme of ^{188}Pb is shown in Fig. 1. Two recent studies have confirmed and extended the previous information on ^{188}Pb , by prompt γ and electron spectroscopy [7] and γ spectroscopy following isomeric decays [14]. In-beam studies making use of the recoil-gating technique have reached beyond the neutron midshell to ^{184}Pb [15] and ^{182}Pb [16]. The prompt in-beam studies of the Pb isotopes around $N=104$ select nearly exclusively the yrast prolate band, and the information on the oblate configuration is mostly limited to the 0^+ “bandhead” seen in α decay. Most of the spherical excitations are also nonyrast, with the exception of long-lived isomers [14]. Even in the mass region where all three configurations (spherical, oblate, prolate) become energetically close, little is known about the magnitude of the mixing between the three structures of different deformation at spins higher than $0\hbar$.

Theoretical studies of the mixing between shape coexisting configurations with significant deformation are quite involved and difficult to perform. Therefore, it is important for our understanding of shape coexistence to extract mixing matrix elements directly from experiment. We have performed a lifetime measurement on ^{188}Pb , with the aim of studying the deformation of the known rotational band of, supposedly, prolate character [7,12,13], and its mixing with the oblate and/or spherical configurations.

II. EXPERIMENTAL DETAILS AND RESULTS

In a pioneering experiment, we have studied the $^{40}\text{Ca}(^{152}\text{Sm},4n)^{188}\text{Pb}$ reaction in inverse kinematics, com-

binning the high granularity and high efficiency for γ -ray detection of the Gammasphere array [17] and the high mass resolution of the Fragment Mass Analyzer (FMA) [18] with the sensitivity of the New Yale Plunger Device (NYPD) [19] for lifetimes in the region of one to several hundreds of picoseconds. The fusion-evaporation reaction $^{40}\text{Ca}(^{152}\text{Sm},4n)^{188}\text{Pb}$ was used with a $800\text{-}\mu\text{g}/\text{cm}^2$ -thick ^{40}Ca target evaporated onto a $900\text{-}\mu\text{g}/\text{cm}^2$ -thick ^{92}Mo backing. The ^{152}Sm beam, with energy of 805 MeV and intensity 1–2 pA, was delivered by the ATLAS accelerator at Argonne National Laboratory. The standard Gammasphere target chamber was replaced by the NYPD [19], which contained the Mo-backed ^{40}Ca target. A degrader foil of $4\text{-mg}/\text{cm}^2$ -thick ^{93}Nb was used in the NYPD, instead of the usual stopper foil, in order to allow the fusion-evaporation products to recoil into the FMA. Evaporation residues were separated by M/q , where M is the mass and q is the charge state of the evaporation residue, and detected at the focal plane of the FMA using two microchannel plate detectors to provide position and timing information and an ion chamber with three segments along the direction of the beam for ΔE - E information. Prompt γ rays were detected by the Gammasphere array in a configuration consisting of 101 large volume, high-purity germanium detectors, each in a bismuth germanium oxide Compton suppression shield, grouped into 16 rings around the target chamber. Detectors belonging to the same ring are positioned at the same polar angle with respect to the beam axis. The overwhelming background generated by fission products was suppressed by selecting only γ rays in coincidence with a recoil at the FMA focal plane. An additional selection using the ΔE - E information was imposed on the particles detected at the focal plane in order to separate the evaporation residues from ^{152}Sm ions accidentally scattered from the beam. A total of 3.6×10^6 events were obtained which satisfy these conditions.

The beam energy in the middle of the target amounted to 730 MeV, resulting in a mean recoil energy after the target of 530 MeV and a recoil velocity of 7.8% of the velocity of light c . The recoils were slowed down to $v/c=5.8\%$ after passing through the Nb degrader and separated from the direct beam and fission products using the FMA at 0° with respect to the beam direction. The velocity of the ^{152}Sm projectiles after the target was $v/c=9.9\%$ and decreased to $v/c=7.9\%$ after the degrader. Recoil-gated γ rays were detected for eight different target-degrader distances, ranging between $\sim 5\text{ }\mu\text{m}$ (just before electrical contact between target and degrader) and $6000\text{ }\mu\text{m}$. All γ rays were Doppler corrected using the value $v/c=5.8\%$ (velocity after the degrader) and the angle corresponding to the ring of Gammasphere in which they were detected. The time of flight of the recoils between target and degrader ranged between a few hundred femtoseconds for the smallest distance and $\sim 300\text{ ps}$ for the largest one. Figure 2 shows a recoil-gated γ -ray projection spectrum for a target-stopper distance of $5\text{ }\mu\text{m}$ (electrical contact), obtained by adding together the spectra of six rings of Gammasphere located at forward angles between 31.7° and 79.2° with respect to the beam direction. Despite the additional gate set on the recoils identified at the focal plane of the FMA, γ rays originating from the Coulomb

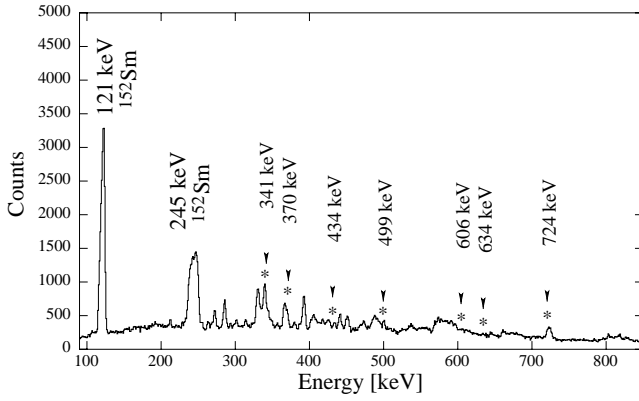


FIG. 2. Recoil-gated γ -singles spectrum obtained by summing together the spectra of the first six rings of Gammasphere. The target-degrader distance is 5 μm . The γ -ray transitions from ^{188}Pb are marked with an asterisk.

excitation of the ^{152}Sm beam are still clearly seen in the spectra as well as background originating from random coincidences.

For the analysis of the experiment, the 16 detector rings of Gammasphere were rearranged, using the Doppler-shift correction for the recoil velocity after the degrader, into forward, backward, and medium polar angle θ groups, corresponding to $\theta \leq 69.8^\circ$, $\theta \geq 110.2^\circ$, and $79.2^\circ \leq \theta \leq 110.2^\circ$, respectively. The recoil-gated coincident γ rays were then sorted into nine matrices at each measured distance according to their registration by the detectors belonging to a pair of particular angular groups. Normalization factors for the data at the different distances were obtained using γ rays following the Coulomb excitation of levels of the ^{152}Sm projectile. The differential decay curve method (DDCM) [20,21] was employed for the lifetime analysis. Referring the reader to Refs. [20,21] for more details, here we only mention the main points as well as features specific to the present work. In the framework of the DDCM, the lifetime of a particular level is determined using only the decay curves of one of the depopulating transitions and those of the direct feeders. This is an important advantage compared to the standard analysis of recoil distance Doppler-shift (RDDS) decay curves (with fitting procedures), where the complete feeding history of the level of interest has to be taken into account in the determination of its lifetime. In its coincidence variant, the DDCM analysis effectively eliminates the uncertainties due to unknown feeding times encountered in the standard RDDS analysis. We have applied this coincidence version for the determination of the lifetime of the 2^+ level in ^{188}Pb (see below). In the present work, to increase the statistics of the coincidence spectra, gates were placed on the full line shapes of the detected γ -ray transitions corresponding to emissions in flight both before and after the degrader, in all three angular groups. This is different from the usual practice of setting gates within the framework of the coincidence version of the DDCM, where the shifted components of the feeding transitions are normally used. Here, the need to increase statistics and the (related) insufficient resolution between the fully shifted and degraded components of the

γ -ray transitions forced us to use the former approach. With the present data, it was possible to determine the lifetimes of the 4^+ and 2^+ levels located at 1065 keV and 724 keV, respectively (Fig. 1). For this purpose, we used the data for the cascade consisting of the 370-, 341-, and 724-keV transitions. In the case of the 4^+ level, spectra at forward and backward angles were used. They were obtained by gating on the 724-keV transition in the matrices at forward, backward, and medium angles. In these spectra, some of which are presented in Fig. 3, the areas of the fully shifted $\tilde{S}(x)$ and degraded $\tilde{R}(x)$ components of the 370- and 341-keV transitions were determined at every distance x by a careful peak fitting procedure. It was found that the 370-keV transition accounts for 62% of the feeding of the 4^+ level. To determine the lifetime τ of this level, we employed the following formula [20,21]:

$$\tau_i = \tau_i(x) = \frac{b_{ij} \frac{\tilde{S}_{ij}(\infty)}{(1 + \alpha_{ij})I_{ij}^\gamma} \sum_h \tilde{S}_{hi}(x) \frac{(1 + \alpha_{hi})I_{hi}^\gamma}{\tilde{S}_{hi}(\infty)} - \tilde{S}_{ij}(x)}{d\tilde{S}_{ij}(x)/dt}. \quad (1)$$

Here, the summation in the numerator runs over all direct feeders h of the level i which is depopulated by the transition $i \rightarrow j$. The quantities b_{lm} are the branching ratios of the transitions $l \rightarrow m$, α_{lm} are the internal conversion coefficients of these γ -ray transitions, I_{lm}^γ are their relative intensities, and $\tilde{S}_{lm}(\infty)$ are the areas of the fully shifted components at the largest distance. [The latter quantities are equal to areas $\tilde{R}_{lm}(0)$ of the degraded peaks at distance $x=0$ μm .] The time derivative $d\tilde{S}_{ij}(x)/dt$ is obtained by fitting piecewise with second-order polynomials the decay curve $\tilde{S}_{ij}(x)$ over an optimized set of time bounds. In this way, Eq. (1) yields a set of values $\tau(x)$ (the so-called τ curve) which should naturally lie on a constant line. Deviations from such behavior immediately indicate the presence of systematic errors in the analysis. In addition, this equation allows for a straightforward calculation of the statistical uncertainty of the mean value of τ_i determined as a mean value of the τ curve within the sensitivity region, i.e., where the numerator and denominator are not too small. To determine the lifetime of the 4^+ level, we summed up the gated decay curves of the 370- and 341-keV transitions at forward and backward angles. Because of the 38% unknown feeding at this state, we had to involve in the analysis an hypothesis about its time behavior. It was assumed that it is similar to the time behavior of the known feeding and, therefore, the sum in the numerator of Eq. (1) was reduced to the decay curve of the 370-keV transition, with an intensity renormalized to that of the 341-keV one (for a more detailed discussion, also on other possible approaches to treating the unknown feeding, see Ref. [20]). The final result of $\tau(4^+) = 16(8)$ ps was derived. For the analysis of the 2^+ level, the decay curve $\tilde{S}(x)$ of the 724-keV transition was obtained by gating similarly to the case of the 4^+ level, but this time on the feeding 341- and 370-keV transitions. The areas of the fully shifted peaks at backward

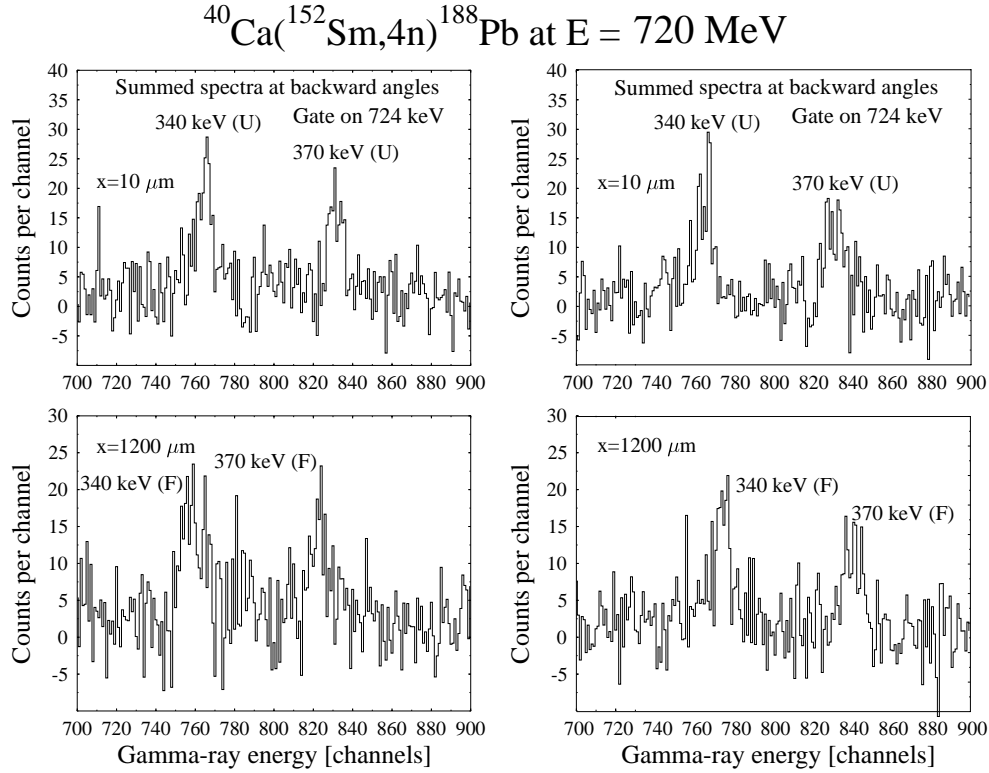


FIG. 3. Recoil-gated γ - γ coincidence spectrum obtained by gating on the 724-keV transition and summing together the spectra of the first (forward) or last (backward) six rings of Gammasphere. The target-degrader distance x is $10 \mu\text{m}$ for the spectra in the upper part of the figure and $1200 \mu\text{m}$ for the spectra in the lower part. The γ -ray transitions from ^{188}Pb are indicated. U and F denote the unshifted and fully shifted components, respectively.

and forward angles were again summed up. The feeding was described by the decay curve of the 341-keV transition, used earlier for the analysis of the 4^+ level and obtained with a gate on the 724-keV γ ray. Thus, the problem of the side feeding was eliminated at the 2^+ level. The effect of modifying the time dependence of the decay curve of the 724-keV transition by using the indirect gate on the 370-keV line compared to the gate on the 341 keV one was found to be small. The final result of the lifetime analysis is $\tau(2^+) = 13(7)$ ps. Figures 4 and 5 illustrate the lifetime determination of the 2^+ and 4^+ levels, respectively.

According to Refs. [22,23], several effects have to be taken into account in the lifetime analysis of RDDS measurements. The influence of solid-angle effects, nuclear deorientation, relativistic aberration, and different detector efficiencies for γ rays emitted in flight at different recoil velocities was considered. For instance, it was found that the solid-angle effects have an appreciable influence on the areas $\tilde{R}_{ij}(x)$ of the degraded peaks at distances above 1 mm. However, the distances at which the lifetimes were determined in the present work within the framework of the DDCM are shorter. The influence of the other effects mentioned above falls within the statistical uncertainties of the derived lifetimes which are, admittedly, quite large due the relatively poor statistics of this pioneering measurement.

From the lifetimes derived in the present work we extracted the reduced $E2$ transition probabilities:

$$B(E2; 2_1^+ \rightarrow \text{g.s.}) = 5(3) \text{ W.u.},$$

$$B(E2; 4_1^+ \rightarrow 2_1^+) = 160(80) \text{ W.u.}$$

III. DISCUSSION

The new transition probabilities measured in this work are important to gain a better understanding of the complex nuclear structure of ^{188}Pb . As already mentioned, a prolate structure was attributed to the rotational band observed in ^{188}Pb on the basis of systematics and theoretical calculations. The $B(E2; 4_1^+ \rightarrow 2_1^+)$ value of 160(80) W.u. determined in this work can be considered as the first direct experimental proof of an underlying collective structure and, thus, supports the previously made assumption. The deformation $\beta = 0.198(48)$ deduced from the $B(E2; 4_1^+ \rightarrow 2_1^+)$ value using the relations

$$B(E2, I \rightarrow I-2) = \frac{5}{16\pi} Q_0^2 \langle IK20 | I-2K \rangle^2 \quad (2)$$

and

$$Q_0 = \frac{3}{\sqrt{5\pi}} ZR_0^2 \beta (1 + 0.16\beta) \quad (3)$$

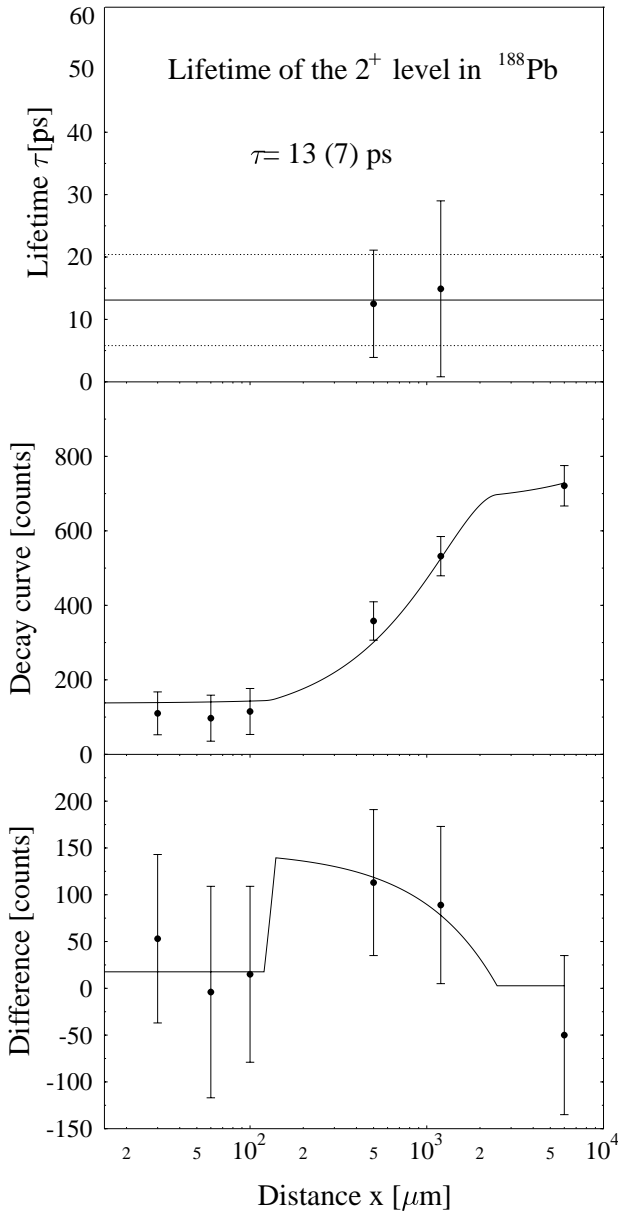


FIG. 4. Determination of the lifetime of the 2^+ level. The panel on the bottom displays the numerator in Eq. (1), i.e., it is the difference of the participating terms. The line drawn through the points is proportional to the time derivative of the decay curve \bar{S} shown in the middle panel. The factor of proportionality is just the value of the lifetime obtained by a simultaneous fit of the difference and the decay curve. Lifetime values calculated at different distances within the sensitivity region are presented in the top panel as well as the mean value of the lifetime and its uncertainty.

is smaller than the theoretical estimates $\beta = 0.26\text{--}0.27$ [10,24,25]. We will come back to this point later in the discussion.

The $B(E2; 2_1^+ \rightarrow \text{g.s.}) = 5(3)$ W.u. is much smaller than the $B(E2; 4_1^+ \rightarrow 2_1^+)$ value and agrees with the value expected for the $E2$ transition strength between spherical states in the lead region [26]. In previous publications, the lowest 2^+ state was considered to be of dominant spherical structure, see, e.g., Refs. [5,27]. Although this interpretation is

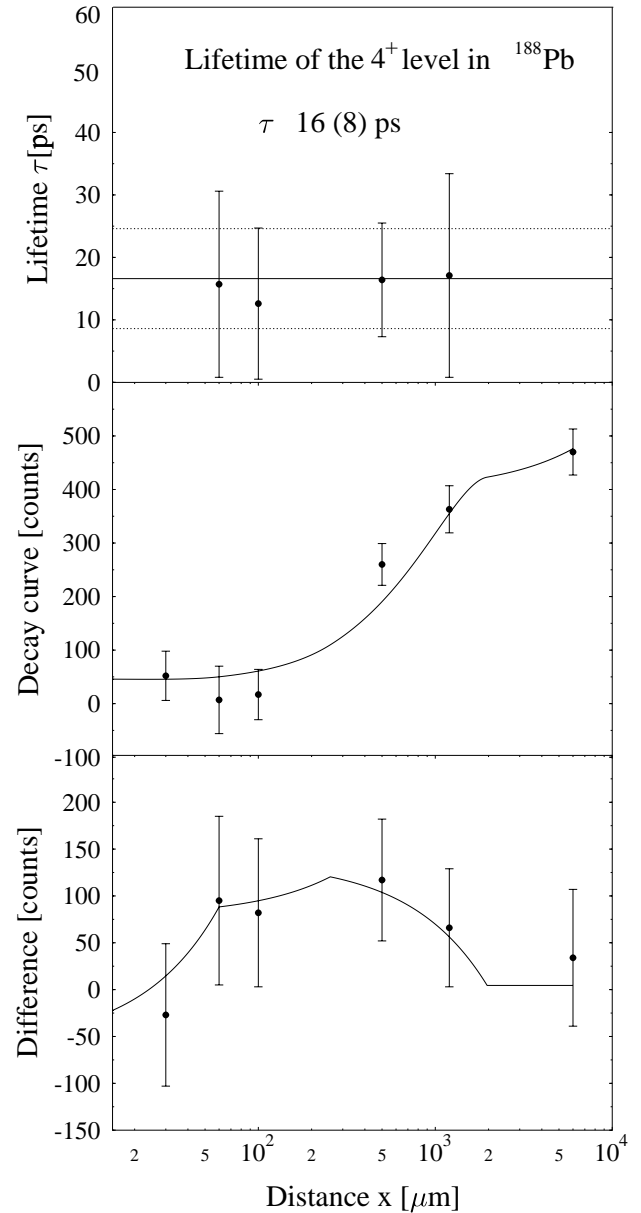


FIG. 5. The same as in Fig. 4, but for the 4^+ state.

consistent with the measured $B(E2; 2_1^+ \rightarrow \text{g.s.}) = 5(3)$ W.u., it is in conflict with the collective $B(E2; 4_1^+ \rightarrow 2_1^+)$ value because the transition from a deformed, presumably prolate [5,12], state (4_1^+ level) to a spherical state is expected to be noncollective and of the order of 1 W.u.

Of course, the three different structures, prolate, oblate, and spherical, can mix and this has an effect on the observed decay patterns. In the following, we use the new experimental data to investigate this issue. Detailed mixing calculations were carried out by Van Duppen *et al.* for 0^+ states of $^{190\text{--}200}\text{Pb}$ [26]. In the case of ^{188}Pb , Allat *et al.* [5] performed three-level mixing calculations in which several assumptions were made because of the rather scarce experimental data. At the time of those studies, only the 0^+ states of all three structures involved in ^{188}Pb were known, and

only the yrast sequence was established at higher spins.

The assumptions used by Allatt *et al.* were as follows: (1) constant mixing strengths as a function of spin, (2) extrapolation of the unmixed deformed states using the Harris parametrization, (3) fit of the used mixing strengths as well as of the unperturbed spherical states, (4) the energies of the unmixed prolate and oblate bandheads were estimated from systematics, e.g., the (2p-2h) systematics.

The results obtained by Allatt *et al.* are not consistent with the large $B(E2;4_1^+ \rightarrow 2_1^+)$ value measured in this work, which indicates that the lowest 2_1^+ state is of dominant prolate character, as well as the higher members of the observed rotational band. At the same time, the deformation extracted from the $B(E2;4_1^+ \rightarrow 2_1^+)$ value is somewhat smaller than the theoretical estimates, which leads one to expect for the 2_1^+ wave function a squared prolate amplitude of 60% and higher. Since this 2^+ state is the lowest observed one, the unmixed spherical and oblate 2^+ levels should lie higher in excitation energy compared to the unmixed prolate 2^+ state. Recently, new experimental data were provided by Dracoulis *et al.* [28]. These authors report on a new, positive parity band, presumably of oblate character. The excitation energy of the 2^+ level was found to be 953 keV. It is depopulated via a strong transition to the ground state and via a 229-keV γ ray to the 2_1^+ state. No transition to an excited 0^+ state has been observed so far. Before we discuss this point in more detail, we have to address the mixing of the 0^+ states.

Experimentally, the situation for the 0^+ levels is much clearer, since three different states have been observed and assigned the respective dominant prolate, oblate, and spherical character by arguments based on the 0^+ systematics observed in neighboring lead nuclei as well as on an analysis of α -decay hindrance factors [3–7]. For ^{188}Pb one finds a sequence of excitation energies $E_{sph} \leq E_{obl} \leq E_{pro}$.

The energy of the unmixed prolate 0^+ state can be estimated by fitting the experimental energies of the band members with the Harris approximation [29], which yields $E_{0_{pro}} = 710$ keV. The unmixed spherical 0^+ state is assumed to be very close to the actual ground state, because it has a relatively large energy difference to the other 0^+ levels. Finally, the position of the unperturbed oblate 0^+ state can be estimated by extrapolating the excitation energies of heavier lead isotopes down to ^{188}Pb . This results in $E_{0_{obl}} \approx 600$ keV. A two-level mixing calculation gives $E_{0_{obl}} = 606$ keV and an oblate-prolate interaction strength of $V_{obl-pro} = 40$ keV with the constraint that the observed 0^+ states are reproduced by the calculation. In this picture, the admixture of deformed configurations into the spherical ground state is assumed to be very small because of the large excitation energy differences. At the same time, a three-level mixing calculation would be rather insensitive toward interaction matrix elements connecting with the spherical state.

A slightly different approach can be taken where, instead of the Harris parametrization, the observed yrast sequence of ^{180}Pt (the corresponding states agree within a few keV with the levels of the band of ^{188}Pb) is used to extrapolate the unperturbed prolate 0^+ state. This procedure results in $E_{0_{obl}} = 626$ keV, $E_{0_{pro}} = 687$ keV, and $V_{obl-pro} = 60$ keV.

Obviously both approaches produce comparable results, a fact that gives confidence in the adopted interpretation as well as some idea about the accuracy of the evaluation of the unperturbed energies and the mixing strength $V_{obl-pro}$.

After having studied the details of the mixing of the 0^+ states, we can turn again to the 2^+ levels. Using the analogy with the yrast sequence of ^{180}Pt , one finds for the unmixed prolate 2^+ state $E_{2_{pro}} = 840$ keV. In order to reproduce our experimental 2_1^+ state with a dominantly prolate character in a three-level mixing calculation, the position of the purely spherical 2^+ level is of crucial importance. A position below the purely prolate state, as suggested in the work of Allatt *et al.* [5], is in contradiction with our experimental assignment of dominantly prolate character to the lowest 2^+ level.

The above argument is supported by the work of Dracoulis *et al.* [28], who, in addition to establishing the oblate state at 953 keV excitation energy, found a candidate for the spherical 2^+ level at an excitation energy of 1109 keV. Using the data specified above, we performed a mixing calculation with the constraint on reproducing the energy of the observed 2^+ states, including the 2^+ level at 1109 keV. Different excitation energies for the unperturbed spherical and oblate 2^+ states were tested in the ranges of 1030–1070 keV and 910–940 keV, respectively. It turned out that the applied constraints determined the interaction strengths fairly well with an accuracy of 10–20 keV. The results of the calculation with the best agreement with the experiment are given in Table I and in Fig. 6.

The excitation energy obtained for the unmixed spherical 2^+ state $E_{2_{sph}} = 1040$ keV is close to the values $E_{2_{sph}} \approx 1060$ –1070 keV determined in Ref. [26] for the heavier Pb isotopes ($A = 190$ –196). The wave function of the lowest 2^+ state has a squared prolate amplitude of 62%, consistent with the measured $B(E2;4_1^+ \rightarrow 2_1^+)$ value of 160(80) W.u. Shortly after this work was completed, we received a preprint of a paper dedicated to ^{188}Pb by Dracoulis *et al.* [30] where a dominant prolate amplitude of $a_{pro}^2 = 69\%$ is also given for the yrast 2^+ state. This value is quite close to our result. Differences appear for the smaller components of the wave

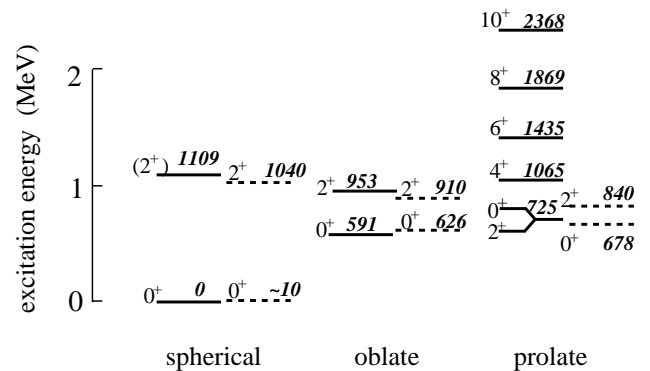


FIG. 6. Experimental and unperturbed levels, represented with solid and dashed lines, respectively, for the low-lying spherical, oblate, and prolate structures in ^{188}Pb . The experimental $0_{2,3}^+$ and $2_{2,3}^+$ states are taken from Ref. [7] and Refs. [28,30], respectively. The energies are given in keV. The details of the three-band mixing calculation are given in Table I and are discussed in the text.

TABLE I. Mixing amplitudes, unmixed, and mixed level energies (in keV) and interaction strengths (in keV) in ^{188}Pb for the first three 2^+ levels. The numbers in the first row of the second column represent the calculated mixed level energies (in keV). For comparison the corresponding experimental values are given in brackets.

Calculation	Experimental levels		
	721 (2_1^+ ; 724 keV)	953 (2_2^+ ; 953 keV)	1116 (2_3^+ ; 1109 keV)
840	0.786	0.441	-0.432
Prolate			
910	-0.019	-0.682	-0.731
Oblate			
1040	-0.617	0.583	-0.528
Spherical			
Interactions	$V_{sph-pro}$ 55	$V_{sph-obl}$ 60	$V_{obl-pro}$ 150

functions which can be easily explained by different assumptions used in the band mixing calculations.

Thus, our calculation accounts for the decrease of this experimental transition strength compared to that expected from the theoretical estimate of the deformation of the unmixed prolate band.

For the oblate-prolate interaction strength $V_{obl-pro} = 150$ keV was determined. This is considerably larger than the corresponding interaction strength $V_{obl-pro} = 60$ keV for the 0^+ states. No solution could be found with approximately equal interaction strengths $V_{obl-pro}$ for the 0^+ and the 2^+ states. We note that spin dependent interaction strengths have been found also in other cases, e.g., mixing of intruder with spherical states [31,32] or superdeformed with normal deformed states [33–36].

Our findings indicate a less developed separation of the oblate and prolate structures in ^{188}Pb at spin $2\hbar$ than at spin $0\hbar$. Different structures separated by a pronounced potential well interact less strongly than those separated by a less developed one. Concerning the interaction strengths of the 0^+ states, we cannot draw any further conclusion since the known experimental data do not allow to fix the corresponding interaction strengths sufficiently well. It will be interesting to compare the new experimental data on ^{188}Pb with more fundamental theoretical approaches which are under development, e.g., Refs. [37,38].

IV. CONCLUSIONS

We have performed a lifetime measurement of the 2_1^+ and 4_1^+ levels in ^{188}Pb using the reaction $^{40}\text{Ca}(^{152}\text{Sm}, 4n)^{188}\text{Pb}$ at 805 MeV. The NYPD was used together with the Gamma-sphere array and the FMA separator. γ rays emitted by the evaporation residues were selected from the overwhelming fission background using the recoil-gating technique.

By means of the RDDS method, the lifetimes of the 2_1^+ and 4_1^+ states of ^{188}Pb were extracted. The deduced transition probabilities show that the band observed in ^{188}Pb is indeed of collective nature with a deformation $\beta \geq 0.17$. The lowest 2^+ state is of dominant prolate character ($a_{pro}^2 = 0.62$). In the framework of a three-band mixing calculation, it is possible to reproduce all known experimental data, including the transition probabilities determined in this work. Lifetime information for band members of higher spin can provide a better insight into the unperturbed structure of the prolate band, and a more reliable mixing picture for the low-spin states.

ACKNOWLEDGMENTS

This work was supported by BMBF (Germany) under Contract No. 06K167, by the U.S. Department of Energy, Nuclear Physics Division, under Contract No. W-31-109-ENG-38, and in part under Grant No. DE-FG02-91ER-40609.

- | | |
|---|--|
| <p>[1] J.L. Wood, K. Heyde, W. Nazarewicz, M. Huyse, and P. Van Duppen, <i>Phys. Rep.</i> 215, 101 (1992).</p> <p>[2] A.N. Andreyev <i>et al.</i>, <i>Nature (London)</i> 405, 430 (2000).</p> <p>[3] N. Bijnens <i>et al.</i>, <i>Z. Phys. A</i> 356, 3 (1996).</p> <p>[4] A.N. Andreyev <i>et al.</i>, <i>J. Phys. G</i> 25, 835 (1999).</p> <p>[5] R.G. Allatt <i>et al.</i>, <i>Phys. Lett. B</i> 437, 29 (1998).</p> <p>[6] R.D. Page <i>et al.</i>, <i>J. Phys. G</i> 25, 771 (1999).</p> <p>[7] Y. Le Coz <i>et al.</i>, <i>EPJdirect</i> 1, 1 (1999).</p> <p>[8] K. Heyde, J. Jolie, J. Moreau, J. Ryckebusch, M. Waroquier, P. Van Duppen, M. Huyse, and J.L. Wood, <i>Nucl. Phys.</i> A466, 189 (1987).</p> | <p>[9] C. De Coster, B. Decroix, and K. Heyde, <i>Phys. Rev. C</i> 61, 067306 (2000).</p> <p>[10] W. Nazarewicz, <i>Phys. Lett. B</i> 305, 195 (1993).</p> <p>[11] J. Wauters <i>et al.</i>, <i>Phys. Rev. Lett.</i> 72, 1329 (1994).</p> <p>[12] J. Heese, K.H. Maier, H. Grawe, J. Grebosz, H. Kluge, W. Meczynski, M. Schramm, R. Schubart, K. Spohr, and J. Styczen, <i>Phys. Lett. B</i> 302, 390 (1993).</p> <p>[13] A.M. Baxter <i>et al.</i>, <i>Phys. Rev. C</i> 48, R2140 (1993).</p> <p>[14] G.D. Dracoulis, A.P. Byrne, A.M. Baxter, P.M. Davidson, T. Kibedi, T.R. McGoram, R.A. Bark, and S.M. Mullins, <i>Phys. Rev. C</i> 60, 014303 (1999).</p> |
|---|--|

- [15] J.F.C. Cocks *et al.*, *Eur. Phys. J. A* **3**, 17 (1998).
- [16] D.G. Jenkins *et al.*, *Phys. Rev. C* **62**, 021302 (2000).
- [17] I.Y. Lee, *Nucl. Phys.* **A520**, 641c (1990).
- [18] C.N. Davids, B.B. Back, K. Bindra, D.J. Hendersen, W. Kutschera, T. Lauritsen, Y. Nagame, P. Sugathan, A.V. Ramayy, and W.B. Walters, *Nucl. Instrum. Methods Phys. Res. B* **70**, 358 (1992).
- [19] See <http://wnsl.physics.yale.edu/structure/equipment/plunger.html>
- [20] A. Dewald, S. Harissopulos, and P. von Brentano, *Z. Phys. A* **334**, 163 (1989).
- [21] G. Böhm, A. Dewald, P. Petkov, and P. von Brentano, *Nucl. Instrum. Methods Phys. Res. A* **329**, 248 (1993).
- [22] K.W. Jones, A. Schwarzschild, E.K. Warburton, and D.B. Fossan, *Phys. Rev.* **178**, 1773 (1969).
- [23] R.J. Sturm and M.W. Guidry, *Nucl. Instrum. Methods* **138**, 345 (1976).
- [24] F.R. Xu, P.M. Walker, J.A. Sheikh, and R. Wyss, *Phys. Lett. B* **435**, 257 (1998).
- [25] F.R. Xu, P.M. Walker, and R. Wyss, *Phys. Rev. C* **59**, 731 (1999).
- [26] P. Van Duppen, M. Huyse, and J.L. Wood, *J. Phys. G* **16**, 441 (1990).
- [27] G.D. Dracoulis, A.P. Byrne, and A.M. Baxter, *Phys. Lett. B* **432**, 37 (1998).
- [28] G. D. Dracoulis, A. P. Byrne, G. J. Lane, A. M. Baxter, T. Kibedi, A. O. Machiavelli, P. Fallon, and R. M. Clark, *Frontiers of Nuclear Structure*, edited by Paul Fallon, AIP Conference Proceedings (to be published).
- [29] G.D. Dracoulis, *Phys. Rev. C* **49**, 3324 (1994).
- [30] G.D. Dracoulis, G.J. Lane, A.P. Byrne, A.M. Baxter, T. Kibedi, A.O. Macchiavelli, P. Fallon, and R.M. Clarke, *Phys. Rev. C* **67**, 051301 (2003).
- [31] J. Gableske *et al.*, *Nucl. Phys.* **A691**, 551 (2001).
- [32] A.M. Oros, K. Heyde, C. De Coster, B. Decroix, R. Wyss, B.R. Barrett, and P. Navratil, *Nucl. Phys.* **A645**, 107 (1999).
- [33] E. Vigezzi, R.A. Broglia, and T. Dossing, *Phys. Lett. B* **249**, 163 (1990).
- [34] R. Krücken, *Phys. Rev. C* **62**, 061302 (2000).
- [35] A. Dewald *et al.*, *Phys. Rev. C* **64**, 054309 (2001).
- [36] A. Dewald *et al.*, in *Proceeding of the International Symposium on Nuclear Structure Physics*, edited by R. Casten, J. Jolie, U. Kneissel, and P. Lieb (Göttingen, Germany, 5–8 March, 2001), p. 311.
- [37] R. Fossion, K. Heyde, G. Thiamova, and P. van Isacker, *Phys. Rev. C* **67**, 024306 (2003).
- [38] N. A. Smirnova, P.-H. Heenen, and G. Neyens (unpublished).